

## SYNTHESIS AND CHARACTERIZATION OF Ag@TiO<sub>2</sub> CORE-SHELL NANOPARTICLES AND STUDY OF ITS ANTIBACTERIAL ACTIVITY

K. I. DHANALEKSHMI, K. S. MEENA & I. RAMESH

PG & Research Department of Chemistry, Queen Mary's College, Chennai, Tamil Nadu, India

### ABSTRACT

Core-shell type Ag@TiO<sub>2</sub> nano particles were prepared by one pot simultaneous reduction of AgNO<sub>3</sub> and hydrolysis of Ti(IV) isopropoxide. They were characterized by absorption, XRD, FTIR, TGA, DSC and HR-TEM techniques. XRD patterns show the presence of anatase form of TiO<sub>2</sub> and the noble metal (Ag). High resolution transmission electron microscopic measurements revealed that their size is below 50 nm. The antibacterial properties of Ag@TiO<sub>2</sub> core-shell nanoparticles against *Escherichia coli* (*E.coli*) and *Staphylococcus aureus* (*S.aureus*) were examined by the agar diffusion method. As a result *E.coli* and *S.aureus* were shown to be substantially inhibited by Ag@TiO<sub>2</sub> core-shell nanoparticles. These results demonstrated that TiO<sub>2</sub> supported on the surface of Ag NPs without aggregation was proved to be a good novel antibacterial activity.

**KEYWORDS:** Core- Shell Nanoparticles, *Escherichia coli*, *Staphylococcus aureus*, Antibacterial Activity

### INTRODUCTION

Antibacterial activity agents are very important in the textile industry, water disinfection, medicine and food packaging. Organic compounds used for disinfection have some disadvantages, including toxicity to the human body, therefore the interest in inorganic disinfectants such as metal oxide nanoparticles is increasing [1]. Inorganic antibacterial agents are superior to organic antibacterial materials in terms of their durability, heat resistance, toxicity, selectivity and various other characteristics [2].

Among the inorganic nanoparticles, silver has been recognized as an effective antimicrobial agent that exhibits low toxicity in human and has diverse in vitro and in vivo application [3]. Ag nanoparticles have attracted considerable attention and have been used as an antibacterial activity and the unlikelihood to develop resistant microorganisms [4,5]. The principal characteristic of Ag nanoparticles is their high surface area to volume ratio, resulting in appearance of new mechanical, chemical, electrical, optical, magnetic, electro-optical, and magneto-optical properties of the nanoparticles that are different from their bulk properties [6]. The antimicrobial activity of Ag nanoparticles is a result of the interaction of silver ions with the three main components of the bacterial cell: the peptidoglycan cell wall and plasma membrane, bacterial DNA and bacterial protein, particularly enzymes [7].

It is widely believed that silver nanoparticles are incorporated in the cell membrane, which causes leakage of intracellular substances and eventually causes cell death [8,9]. Some of the silver nanoparticles incorporated, also penetrate into the cells. The antimicrobial activity increases with decreasing size of the Ag nanoparticles [10]. But Ag nanoparticles with diameter less than 200 nm tend to aggregate spontaneously, and their stability in air, water, or sunlight is not good enough for long term applications [11], which will decrease their antibacterial performance. To solve this problem, a wide range of materials TiO<sub>2</sub> [12], SiO<sub>2</sub> [13], Al<sub>2</sub>O<sub>3</sub> [14], zeolites [15] and activated carbon fibres [16] have been employed to support Ag nanoparticles, so that the ultra fine Ag nanoparticles can be homogeneously formed without aggregation [17].

Among the various oxide semiconductors, titania has proven to be the most suitable for widespread environment application for its high chemical stability, non-toxicity, low cost and excellent degradation for organic pollutants [18-21]. TiO<sub>2</sub> nanoparticles are easy to attach to the cell membranes and accumulate [22].

The core-shell composite structures, as a kind of new nanostructures, have received intense attention due to their improved physical and chemical properties over their single components, and thus many efforts have been made to synthesize such special core-shell nanostructures [23,24]. The core-shell composite has many advantages as antibacterial agent, such as high antibacterial activity, low toxicity, chemical stability, long lasting action period and thermal resistance versus organic antibacterial agents [25]. In an earlier report it has shown that Ag nanoparticles deposited on TiO<sub>2</sub> nanostructures enhance their bacterial property [26]. Such a structure, through effective, results in exposing both metal Ag to reactants and the surrounding medium. The Ag core-shell nanoparticles would provide a new possibility to be good candidates for antibacterial materials due to their unique structures and at the same time the shell to protect Ag nanoparticles and stabilize them against chemical corrosion. It could be reasonably envisioned that Ag cores would release Ag ion slowly through the outer porous coating layer, thereby producing and maintaining the excellent antibacterial effects [27].

In this study, Ag@TiO<sub>2</sub> core-shell NPs was synthesized and characterized by absorption, XRD, FTIR, TGA, DSC and HR-TEM techniques. The antibacterial activity of the as prepared Ag@TiO<sub>2</sub> core-shell NPs was also examined against *E.coli* and *S.aureus*.

## MATERIALS AND METHODS

### Reagents

Titanium (iv) isopropoxide was purchased from Sigma Aldrich. AgNO<sub>3</sub> was obtained from Merck and all the other chemicals used were of Analar grade. The water used was of Milli-Q type.

### Synthesis of Ag@TiO<sub>2</sub> Core-Shell Nanoparticles

The core-shell type Ag@ TiO<sub>2</sub> was prepared by slight modification of the method described in literature [28]. In brief 20 mM each of Ti (IV) isopropoxide and acetylacetone in 30ml of isopropanol was prepared by sonicating the mixture for 15 minutes. 10 mM solutions of AgNO<sub>3</sub> in 5ml of milli-Q water was prepared and 20ml of DMF was added to it and stirred well. To this solution 30ml of the above sonicated solution was added and stirring continued for 10 more minutes. The final mixture was refluxed between 60 - 70°C for 1 hour. The solution became greenish black and the refluxing was continued for 1 more hour. The precipitate obtained was sonicated for 2 hours to disperse. On adding toluene the colloidal material was precipitated and washed several times with toluene and redissolved in isopropanol. The solvent was evaporated at room temperature to get a greenish black powder of Ag@TiO<sub>2</sub> core-shell nanoparticles.

### Characterization

UV-visible spectra were recorded in a spectrophotometer (Perkin Elmer Lambda 35). FTIR spectroscopic measurements were carried out with a Perkin Elmer FTIR Spectrum RXI spectrometer. Thermogravimetric analysis (TGA) was performed using WATERS SDT Q600 thermal analysis instrument. About 10-20 mg of sample was used at a heating rate of 10° C /min and the data were collected between 35 and 1000°C. The measurements were made in N<sub>2</sub> atmosphere. DSC measurements were carried out in a WATERS DSC Q10 Differential Scanning Calorimeter in oxygen. High resolution transmission electron microscopy (HRTEM) photographs were taken using a JEOL JEM -3010 Electron microscope operating at 300 keV. The magnifying power used was 600 and 800k times.

### Antibacterial Activity Test

The *in vitro* antibacterial activity of Ag@TiO<sub>2</sub> core-shell NPs were tested against the bacterial species *S. aureus*, and *E. coli* by agar diffusion method [29]. Initially, the stock cultures of bacteria were revived by inoculating in broth media and grown at 37 °C for 18 hrs. The agar plates of media (peptone-10 g, NaCl-10 g and yeast extract 5 g, agar 20 g in 1000 ml of distilled water) were prepared and wells were made in the plate. Each plate was inoculated with 18 h old cultures (100 µl) and spread evenly on the plate. After 20 minutes, the wells were filled with compound at 100, 200, 300, 400, 500 and 600 µg/mL concentrations, to determine the minimum inhibitory concentration (MIC) value. All the plates were incubated at 37 °C for 24 h and the diameter of inhibition zone were noted.

## RESULTS AND DISCUSSIONS

### UV-Visible Spectral Analysis

The absorption spectrum of Ag@TiO<sub>2</sub> is shown in Figure 1. It has a broad band centered at 425nm. However it is reported that the plasmon absorption band of the small Ag particles prepared using borohydride reduction is around 380 nm. The red shift in the Ag@TiO<sub>2</sub> spectrum may be due to increase in the particle dimension and /or change in the dielectric constant of the surrounding matrix upon encapsulation.[28].

### XRD Analysis

Standard X-ray powder diffraction was used to determine the identity, relative proportion and average grain size of the core-shell nanoparticles. Figure (2a & 2b) shows the X-ray diffraction pattern of pre and post annealed Ag@TiO<sub>2</sub> (at 650°C in air for 5hrs) respectively. The Figure 2(a) shows that the air dried Ag@TiO<sub>2</sub> core-shell nanoparticle is fully amorphous since there is no peak corresponding to TiO<sub>2</sub> and Ag. The Figure 2(b) shows 4 characteristic peaks of nanocrystalline pure Ag@TiO<sub>2</sub> of monoclinic structure (JCPDS # 52-1202). The major diffraction intensity peaks at 2θ, about 25.42, 32.182, 37.995, 47.839° were identified to originate from (220), (420) (112) and (040) planes of Ag@TiO<sub>2</sub> respectively. The XRD patterns could be indexed to the C2/c (15) space group, end centered monoclinic structure with cell parameters a = 16.77, b = 7.594, c = 5.044 and β = 102.01. Absence of peaks in Figure 2(a) and appearance of these peaks in Figure 2(b) clearly establishes the sintering of both TiO<sub>2</sub> particles to produce bulk dimension. Generally formation of rutile phase is a common thing during calcination. The patters are very well comparable to those reported in literature [28].

### FTIR Spectrum

The FTIR spectrum of Ag@ TiO<sub>2</sub> is shown in Figure 3. The air dried sample of Ag@TiO<sub>2</sub> shows no characteristic peaks due to DMF. The defective OH vibrations below 3500cm<sup>-1</sup>, OH stretch of water at 3362cm<sup>-1</sup>, the OH<sub>2</sub> bend at 1625.1cm<sup>-1</sup> and 531 cm<sup>-1</sup> for the Ti-O stretching, vibration are observed. In addition there are peaks at about 1114cm<sup>-1</sup> and 1382cm<sup>-1</sup> and these peaks are assigned to alkoxide C-O and CH<sub>2</sub> bending vibrations respectively. Hence alcohol might be adsorbed on the surface. The CH<sub>2</sub> stretching vibrations which generally occur just below 3000cm<sup>-1</sup> are not well resolved in this figure. The FTIR spectrum is very well comparable to that reported in literature [28].

### Thermo Gravimetric Analysis (TGA)

The thermo gravimetric analysis of nano Ag@TiO<sub>2</sub> was carried out between 50 and 900°C at a heating rate of 10°C/min in nitrogen atmosphere. The traces of thermogram are illustrated in Figure 4. The mass loss on ignition was related to the content of volatile components, especially physi or chemisorbed water. There is a weight loss between 50 and 125°C due to desorption of adsorbed water. There is a weight loss above 200°C. It involves condensation of defective-OH groupings and oxidation of adsorbed organics on the surface. There is a weight loss above 550°C due to condensation of

difficultly condensable groupings and / or oxidation of organic residues. Thus the thermo gravimetric study of Ag@TiO<sub>2</sub> core-shell nanoparticles shows a monotonous mass decrease with temperature.

### Differential Scanning Colorimetry (DSC)

The DSC analysis of the air-dried Ag@TiO<sub>2</sub> core-shell nanoparticles was carried out between 50 and 400°C at a heating rate of 10°C/min in nitrogen atmosphere. The DSC trace of Ag@TiO<sub>2</sub> is shown in Figure 5. There is an endothermic peak between 50 and 250°C. This endothermic peak coincides with the second major weight loss in the TGA traces shown in Figure 4. The energy changes in this process are also comparable with the percentage weight loss in TGA. There is an exothermic peak between 300 and 400 °C. This may be due to the crystallization of Ag@TiO<sub>2</sub> at this temperature which is in accordance with XRD results shown in Figure 4b. This sharp peak at this higher temperature may presumably involve some form of structural modifications within the Ag@TiO<sub>2</sub> lattice.

### High Resolution Scanning Electron Microscopy (HR-TEM)

The HR-TEM images of Ag@TiO<sub>2</sub> are shown in Figure 6(a-c). The images show a majority of dark images of Ag core in the size regime. Figure 6(a). Illustrates the formation of nearly spherical particles of silver core with particle diameter of 15nm to 20nm and a range of particle morphologies are seen. Although most of the particles seen in this image are spherical or oval, faceted structures were also observed. All of them appear to be associated with TiO<sub>2</sub> shell. The boundary between core (Ag) and shell (TiO<sub>2</sub>) is very much distinct Figure 6 (b-c). HR-TEM image of single Ag@TiO<sub>2</sub> particle is illustrated in Figure 6(b & c). This image illustrates that each particle has a thin capping of TiO<sub>2</sub> shell of thickness in the range 2 to 3nm. Figure 6(a) illustrates aggregation of fine particles of Ag represented by dense regions and associated TiO<sub>2</sub>.

Microscopy reveals no free particles of either silver or oxide. The presence of completely covering shells is confirmed with reactivity studies as well. Capping of TiO<sub>2</sub> shell on the Ag core was confirmed by checking the stability in an acidic solution (HNO<sub>3</sub>). The Ag cluster, stabilized by citric acid, is readily dissolved in an acidic solution (pH=2). Ag@TiO<sub>2</sub> on the other hand is quite stable in HNO<sub>3</sub> solution even when the TiO<sub>2</sub> shell is thin. If the formation of TiO<sub>2</sub> clusters in DMF was independent such that both clusters are formed separately or in the form of a TiO<sub>2</sub>/Ag sandwich structure we would have observed dissolution of Ag clusters. The stability test in acidic solution asserts the argument that the TiO<sub>2</sub> shell on the Ag core is uniform and provides the protection against acid induced corrosion [30].

### Antibacterial Activity of Ag@TiO<sub>2</sub> Core-Shell Nanoparticles

The inhibition zone values were determined for Ag@TiO<sub>2</sub> core-shell NPs were tested against two types of bacteria *E.coli* and *S.aureus* results are shown in the Figure 7. The MIC observed in this study for Ag@TiO<sub>2</sub> core-shell NPs are 100 µg/ml for *S.aureus* and 200 µg/ml for *E.coli*.

The obtained data demonstrates that all the investigated Ag@TiO<sub>2</sub> core-shell NP had relatively high antibacterial activity against Gram negative (*E.coli*) bacteria as compared to that of Gram positive (*S.aureus*) bacteria. The antibacterial activity increases as the concentration of core-shell increases.

The inhibition zone of *S.aureus* is smaller than for *E.coli*. It has been known, that the structure of gram positive and gram negative cell wall has different compositions. The layer of peptidoglycan in gram positive bacteria is thicker than for gram negative bacteria which consequently decrease the penetrations of NPs to the cell wall of gram positive bacteria.

Ag NPs shows three different way of mechanism of action.

Firstly, Ag NPs attach to the surface of the cell membrane and disturb its power functions. Such as permeability and respiration [31]. It is reasonable to state that the binding of the particles to the bacteria depends on the interaction of the surface area available.

Secondly Ag NPs are able to penetrate the bacteria and cause further damage, possibly by interacting with sulfur and phosphorus containing compounds such as DNA [32]. In addition, it is believed that Ag NPs after penetration into the bacteria have inactivated their enzymes, generating hydrogen peroxide and causing bacterial cell death [32,33].

Third, Ag NPs release silver ions, which made an additional contribution to the bactericidal effect [34]. The Ag NPs also contain micro molar concentration of Ag<sup>+</sup> and they have shown that Ag<sup>+</sup> and Ag<sup>0</sup> both contribute to the antibacterial activity. The mechanism of inhibition by silver ions on micro organism is partially known. It is believed that DNA loses its replication ability and cellular proteins become inactivated on silver ion treatment [35]. Higher concentrations of Ag<sup>+</sup> ions have been shown to interact with cytoplasmic components and nucleic acids [34].

It could be concluded that Ag ions from Ag cores could be released through porous TiO<sub>2</sub> shells. It may be reasonable to presume that such core/shell structures will benefit preventing corrosion and prolonging the release time of Ag ions and preserving the sustained antibacterial behavior [36].

Therefore such Ag@TiO<sub>2</sub> core-shell nanoparticles could be useful and effective in bactericidal applications, and would present a reasonable alternative for the development of new bactericides.

## CONCLUSIONS

Ag@TiO<sub>2</sub> core-shell nanoparticles were successfully prepared and their structure were analyzed by techniques such as UV-vis spectroscopy, XRD, FTIR, TGA, DSC and HR-TEM. Positively charged silver reacted easily with gram negative bacteria rather than gram positive bacteria could be selectively killed by the Ag@TiO<sub>2</sub> core-shell NPs more effectively. The core-shell NPs showed good antibacterial activities because TiO<sub>2</sub> deposited on the surface of Ag NPs prevent aggregation. Such core-shell NPs could have promising application as antibacterial materials for microbiocides and water treatment.

## REFERENCES

1. Hajipour et al, Antibacterial properties of nanoparticles.
2. Q.X.Li, H.A.Tang, Y.Z.Li, M.Wang, L.F.Wang, C.G.Xia, J.Inorg.Biochem.78 (2000) 167-174.
3. Farooqui, M.D.A, Chauhan, P.S., Krishanmoorthy, P and Shaik, J .Extraction of Ag Nanoparticles from the leaf extracts of Clerodendrum inerme, Digest Journal of nanomaterials and biostructures, 2010; 5:43-49.
4. V.K.Sharma, R.A.Yngard, Y.Lin, Silver nanoparticles: green synthesis and their antimicrobial activities, Advances in colloid and Interface Science 145 (2009) 83-96.
5. Q.Li, S. Mahaendra, D.Y. Lyon, I. Brunet, M.V. Liga, D. Li, P.J.J. Alvarez, Antimicrobial nanomaterials for water disinfection and microbial control: potential applications and implications, Water research 42 (2008) 4591-4602.
6. Whitesides, G.M. (2005) Nanoscience, nanotechnology, and chemistry. Small 1,172-179.
7. K.Chaloupka, Y. Malam, A.M. Seifalian, Trends Biotechnol.28 (2010) 580.

8. Sondi I, Salopek-Sondi B. Silver nanoparticles as antimicrobial agent: a case study on *E.coli* as a model for gram-negative bacteria. *J.Colloid Interf Sci*-2004;223:313-9.
9. Cho K, Park J, Osaka T, Park S. The study of antimicrobial activity and preservative effects of nanosilver ingredient. *Electrochim Acta* 2005;51:5255-62.
10. C. Baker, A. Pradhan, L. Pakstis, D.J. Pochan, S.I. Shah, J. Nanosci. Nanotechnol.5 (2005) 244.
11. Shunsheng Cao, Juanrong Chen, Jie Hu, Aust. J. Chem. 62 (2009) 1561-1576.
12. O.Akhavan, Lasting antibacterial activities of Ag-TiO<sub>2</sub>/Ag/a-TiO<sub>2</sub> nanocomposite thin film photocatalysts under solar light irradiation, *J. Colloid Interface Sci.*336 (2009) 117–124.
13. S.D. Oh, S.H. Lee, S.H. Choi, I.S. Lee, Y.M. Lee, J.H. Chun, H.J. Park, Synthesis of Ag and Ag-SiO<sub>2</sub> nanoparticles by  $\gamma$ -irradiation and their antibacterial and antifungal efficiency against *Salmonella enterica* serovar Typhimurium and *Botrytis cinerea*, *Colloids Surf. A: Physicochem. Eng. Aspects* 275 (2006) 228–233.
14. Q.Y. Chang, L.Z. Yan, M.X. Chen, H. He, J.H. Qu, Bactericidal mechanism of Ag/Al<sub>2</sub>O<sub>3</sub> against *Escherichia coli*, *Langmuir* 23 (2007) 11197–11199.
15. Y. Inoue, M. Hoshino, H. Takahashi, T. Noguchi, T. Murata, Y. Kanzaki, H. Hamashima, M. Sasatsu, Bactericidal activity of Ag-zeolite mediated by reactive oxygen species under aerated conditions, *J. Inorg. Biochem.* 92 (2002) 37–42.
16. S.X. Chen, J.R. Liu, H.M. Zeng, Structure and antibacterial activity of silver supporting activated carbon fibers, *J. Mater. Sci.* 40 (2005) 6223–6231.
17. Y.H. Kim, D.K. Lee, H.G. Cha, C.W. Kim, Y.S. Kang, Synthesis and characterization of antibacterial Ag-SiO<sub>2</sub> nanocomposite, *J. Phys. Chem. C* 111 (2007),3629–3635.
18. M. Ksibi, S. Rossignol, J.M. Tatibouet, C. Trapalis, Synthesis and solid characterization of nitrogen and sulfur-doped TiO<sub>2</sub> photocatalysts active under near visible light, *Mater. Lett.* 62 (2008) 4204–4206.
19. W.P. Wang, J.L. Zhang, F. Cheng, D. He, M. Anpo, Preparation and photocatalytic properties of Fe<sup>3+</sup>-doped Ag@TiO<sub>2</sub> core-shell nanoparticles, *J. Colloid Interf. Sci.* 323 (2008) 182–186.
20. Q.H. Zhang, W.G. Fan, L. Gao, Anatase TiO<sub>2</sub> nanoparticles immobilized on ZnO tetrapods as a highly efficient and easily recyclable photocatalyst, *Appl. Catal. B* 76 (2007) 168–173.
21. J.G. Yu, X.J. Zhao, Q.N. Zhao, Effect of surface structure on photocatalytic activity of TiO<sub>2</sub> thin films prepared by sol-gel method, *Thin Solid Films* 379 (2000) 7–14.
22. Cai et al., Photokilling of Malignant cells with ultrafine TiO<sub>2</sub> powders, *Bull. Chem. Soc., Jpn* 64, (1991) 1268
23. M.E. Ahmed, Y. Shu, S. Tsugio, *J. Colloid Interface sci.* 300 (2006) 123.
24. M. Bonini, a. Wiedenmann, P. Baglioni, *Mater. Sci. Eng. C*26 (2006) 745.
25. E.C. Antonio, P. Carlos, A. Eduardo, S. Julio, M.J. Antibacte. *J. Mater. Sci.*41 (2006) 5208.
26. Zhang, H.J.; Chen, G.H. *Environ.Sci.Technol.*2009,43,2905.
27. Yue lin, Wang Qiqiang, Zhang Xiaoming, Wang Zhouping, Xia Wenshui, and Dong Yuming. *Bull. Korean Chem. Soc.* 2011, Vol.32, No. 2607.

28. T. Renjis, A. Tom, SreeKumaran Nair, M. Navinder Singh, Aslam, C.L. Nagendra, Reji Philip, K. Vijaya Mohanan and T. Pradeep, Freely Dispersible Au@TiO<sub>2</sub>, Au@ZrO<sub>2</sub>; Ag@TiO<sub>2</sub> and Ag@ZrO<sub>2</sub> Core-Shell Nanoparticles: One-Step Synthesis, Characterization Spectroscopy and Optical Limiting Properties. *Langmuir*, 19, (2003), 3439-3445
29. E. J. Threlfall, I. S. T. Fisher, L. Ward, H. Tschape, P. Gernersmidt, *Microb. Drug Resist.* 5 (1999) 195-199.
30. Tsutomu Hirakawa and Prashant V. Kamat, Charge Separation and Catalytic Activity of Ag@TiO<sub>2</sub> core-shell Composite Clusters Under Uv-irradiation, *J. Am. Chem. Soc.* XXXX, XXX, A-G.
31. Murray, R. G. E., Steed, P. & Elson, H. E. (1965) "The location of the mucopeptide in sections of the cell wall of Escherichia coli and other gramnegative bacteria," *Can. J. Microbiol.* 11, 547-560.
32. M. Raffi, F. Hussain, T. M. Bhatti, J. I. Akhter, A. Hameed, M. M. Hasan, *J. Mater. Sci. Technol.* 24, 192 (2008).
33. Shockman GD, Barrett JF, Structure , function and assembly of cellwalls of gram +ive bacteria. *Annu Rev. Microbiol.* 1983;37:501-27.
34. Feng et.al , A mechanistic study of the a.bact effect of Ag ions on *E.coli* and *S.aureus*. 2000,662-668.
35. P. Gupta , M. Bajpai and S. K. Bajpai. Investigation of Antibacterial Properties of Silver Nanoparticle-loaded Poly (acrylamide-co-itaconic acid)-Grafted Cotton Fabric. *The Journal of Cotton Science* 12:280–286 (2008).
36. Lin et al Synthesis of Ag@TiO<sub>2</sub> core-shell nanoparticles with antibacterial properties, *Bul.Korean chem..soc.* 2011, Vol.32, No.8,2607

## APPENDICES

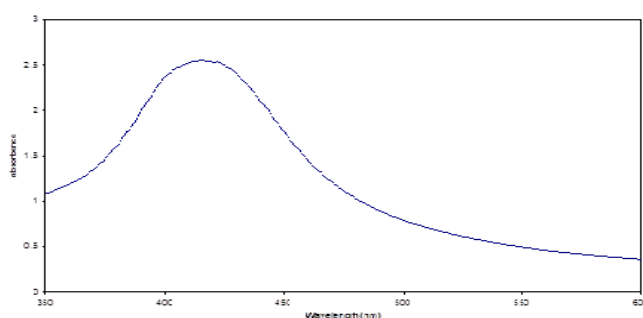


**Figure 1: UV-Vis Spectra of Ag@TiO<sub>2</sub> Core-Shell NPs**

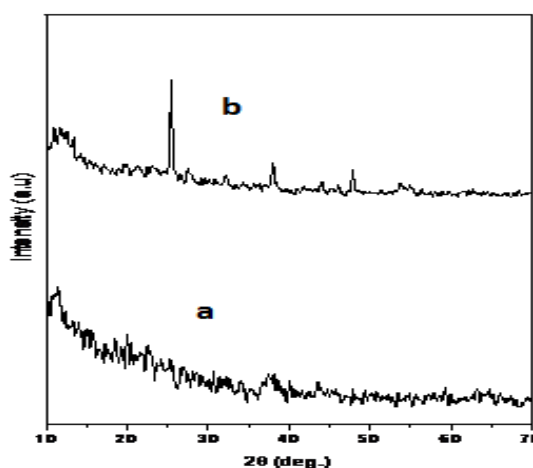


**Figure 2: XRD Spectrum of Ag@TiO<sub>2</sub> Core-Shell NPs a) Air Dried Sample and b) Sample Annealed at 650° C**

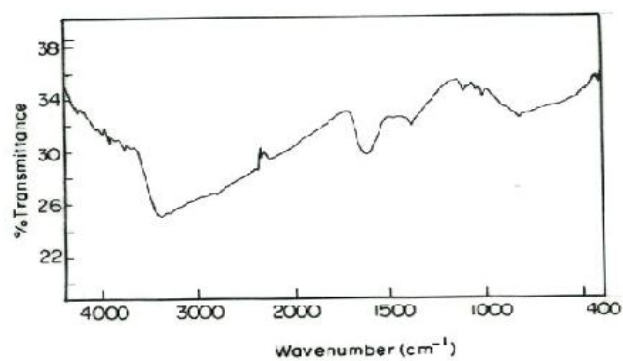


Figure 3: FT-IR Spectra of Ag@TiO<sub>2</sub> Core-Shell NPs

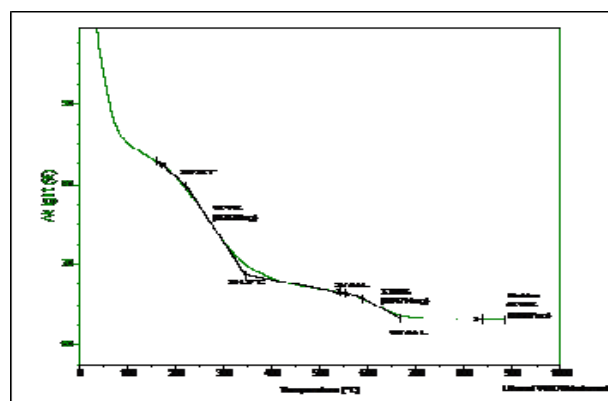


Figure 4: TGA Thermogram of Ag@TiO<sub>2</sub> Core-Shell NPs

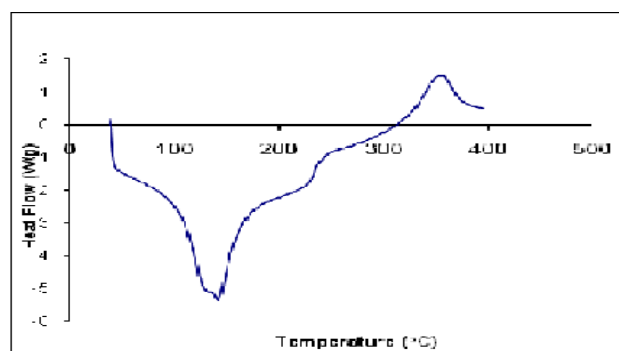
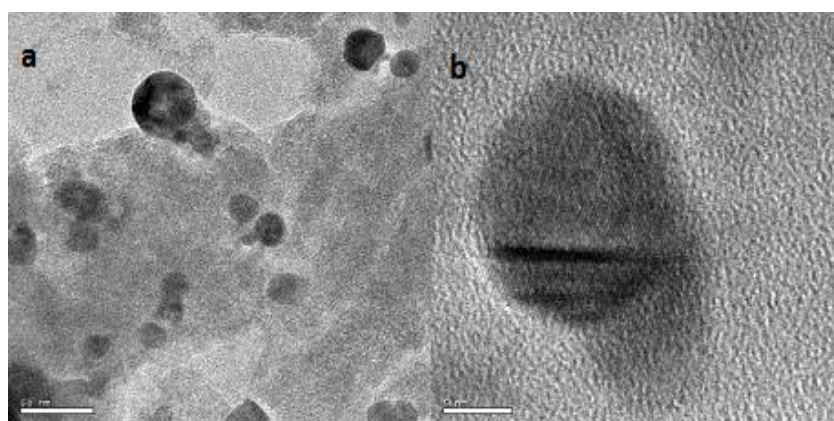


Figure 5: DSC Thermogram of Ag@TiO<sub>2</sub> Core-Shell NPs





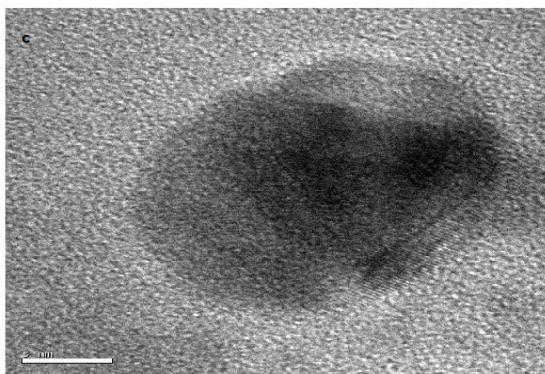


Figure 6: a,b and c-HR-TEM Images of Ag@TiO<sub>2</sub> Core-Shell NPs

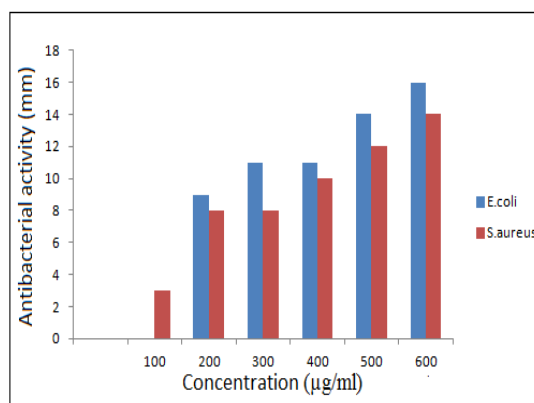


Figure 7: Antibacterial Activity of Ag@TiO<sub>2</sub> Core-Shell NPs

